



Simulated microgravity activates  
MAPK pathways in fibroblasts cultured on  
microgrooved surface topography

WA Loesberg, XF Walboomers, JJWA van Loon and JA Jansen

Cell Motil Cytoskeleton, *in press*, 2008

## INTRODUCTION

For fibroblasts, mechanical stress is an important and specific director of cell shape and stimulus for extracellular matrix component production. For instance, stress provided by a microgrooved pattern onto which the cells are seeded, as well as, stresses from substratum deformation are well documented [1-9]. On the other hand, cells can also experience mechanical unloading by removing the, at cell level, very weak, but ever present force in nature: gravity. Morphological and functional studies have shown that many cells like osteoblast-like cells and lymphocytes are highly sensitive to altered gravity conditions [10-17]. Although it is generally accepted that the response to environmental stimuli is multi-factorial in origin, research towards the interaction of cells cultured on substratum texture (nano-, micropatterns) and mechanical force is sparse. Such studies are necessary to serve as baseline values for further research aimed at understanding of observed cell response phenomena on a molecular basis [18-22]. For instance, what signalling cascades are important in mediating the cellular response (e.g. mRNA expression; cytoskeleton (de)polymerisation) towards their environment. A familiar signalling pathway is the mitogen activated protein kinase (MAPK) pathways which transmits environmental signals from the cell membrane to the nucleus through phosphorylation cascades, resulting in gene expression regulation (**Figure 1**). Three subgroups of MAPKs are known: extracellular signal-regulated kinases (ERK1/2), jun N-terminal kinase/stress-activated protein kinase (JNK/SAPK), and p38<sup>MAPK</sup> (p38). Although it has been shown that these kinases respond to a range of stimuli, little is known about the cellular response to altered gravity circumstances [23-26]. Upstream from ERK1/2 and JNK/SAPK is a family of proteins commonly known as Rho GTPases. Members include, besides Rho, Rac and Cdc42. Rho mediates the formation of cytoskeletal stress fibres, while Rac mediates the formation of membrane ruffles, and Cdc42 mediates the formation of peripheral filopodia. Rho exerts its distinct actions through interactions with ROCK, a serine/threonine protein kinase. Cdc42/Rac operates via p65 activated kinase (PAK). While separate Cdc42/Rac and Rac/Rho hierarchies exist, these might not extend into a linear form since Cdc42 and Rho activities are competitive. ROCK promotes the formation of Rho-induced actin stress fibres and focal-adhesion complexes, to which the ends of the stress fibres attach. On the other hand, Cdc42-induced peripheral filopodia formation is accompanied by Rac-induced membrane ruffles, which together with PAK, which stimulates the disassembly of stress fibres, play a role in cell movement. PAK also fosters loss of focal-adhesion complexes [27-30]. This cooperation and antagonism between different Rho GTPases in their role of reorganisation of the actin cytoskeleton under microgravity has received little attention.

Ground based research to simulate microgravity by means of a Random Positioning Machine (RPM) provides excellent means to conduct gravitational studies. The RPM is a microweight (microgravity) simulator that is based on the principle of 'gravity-vector-averaging'. Gravity is a vector, *i.e.* it has a magnitude and direction. During an experimental run in the RPM the sample position with regard to the Earth's gravity vector is constantly and randomly changing, and as a result the samples will experience a simulated weightlessness environment [31-34].

In this study we evaluated *in vitro* the differences in morphological behaviour between fibroblast cells cultured on polystyrene substrata, both planar and with a surface microtopography, which were placed in a simulated microgravity environment. In addition, the mRNA transcription of several proteins involved in cell-surface interaction was investigated. The underlying aim was to understand which parameter is more important in determining cell response. Our hypothesis is that cellular shape and orientation is determined by the topographical cues, and a simulated microgravity environment will decrease the cellular orientation to these substrata. As control fibroblast cells were cultured on similar substrata, which remained at normal (Earth) gravity.

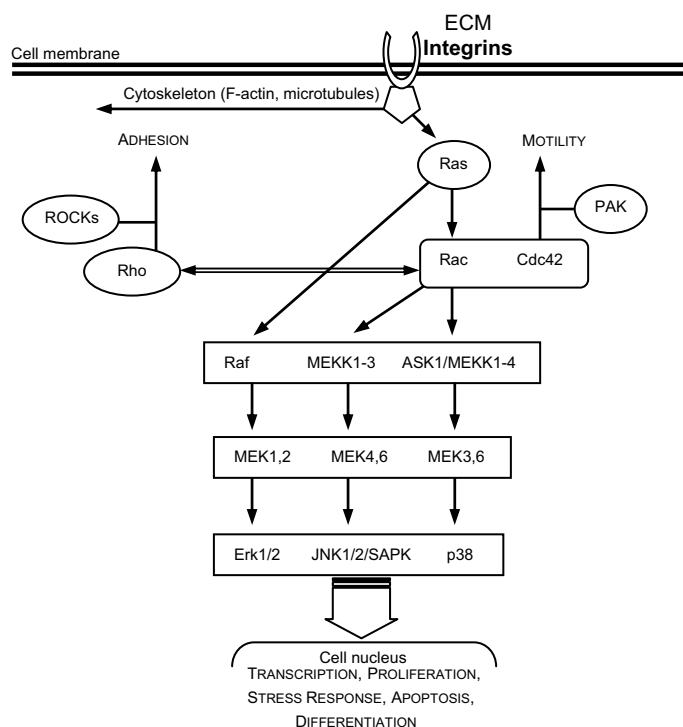


Figure 1. Mitogen Activated Protein Kinases (MAPK) intracellular signalling pathways. A simplified schematic of the three major MAPK pathways and the members of the Rho family of small GTPases.

## MATERIALS AND METHODS

### Substrata:

Microgrooved patterns were made, using a photo lithographic technique and subsequent etching in a silicon wafer as described by Walboomers *et al.* [1]. The dimensions of the microgrooved topography were a ridge- and groove width of 1  $\mu\text{m}$ ; with a uniform depth of 0.25  $\mu\text{m}$ . Wafers with a planar surface were used as controls. The silicon wafer was used as template for the production of polystyrene (PS) substrata for cell culturing. PS substrates were solvent cast in a manner described by Chesmel and Black [35] and were attached to 18 mm diameter cylinders with polystyrene-chloroform adhesive. Shortly before use a radio frequency glow-discharge (RFGD) treatment was applied for 5 minutes at a pressure of  $2.0 \times 10^{-2}$  mbar and a power of 200 W (Harrick Scientific Corp., Ossining, NY, USA) in order to sterilize the dishes, as well as, promote cell attachment by improving the wettability of the substrata.

### Cell culture:

Rat dermal fibroblasts (RDF) were obtained from the ventral skin of male Wistar rats as described by Freshney [36]. Cells were cultured in  $\text{CO}_2$ -independent  $\alpha$ -MEM containing Earle's salts (Gibco, Invitrogen Corp., Paisley, Scotland), L-glutamine, 10% FCS, gentamicin (50 $\mu\text{g}/\text{ml}$ ), in an incubator set at 37  $^\circ\text{C}$  with a humidified atmosphere. Experiments were performed with 4 - 8th culture generation cells. Onto the various substrata,  $1.5 \times 10^4$  cells/ $\text{cm}^2$  were seeded. Cells were pre-cultured for 4h, after which they were placed in a 12 wells plate for support. Custom made silicone caps closed each well and the tissue culture dish therein (**Figure 2**). Using a type 22G1 needle and applying a little pressure while adding additional medium, air bubbles were removed to prevent unwanted shear force and turbulence during rotation in the RPM. In this system with only one specific density fluid and absence of air bubbles no fluid motion was to be expected, since the media was moving with the same velocity as the cell monolayer. The well plates containing the samples were secured onto the platform. From previous studies it is known that fibroblasts need approximately 4 hours to begin adapting their morphology to a new environment [37]. Therefore experimental times were chosen of 30 and 120 minutes and 48 hours to obtain

information on the cell behaviour from an early time period until a state of equilibrium between the cells and their environment.



Figure 2. At left a graphical cross section of a polystyrene culture dish used in this study with silicone closing cap securing the insert snug into the well of a 12 wells plate and providing an air bubble free environment. On the right the Random Positioning Machine (RPM) used in this study to simulate weightlessness. The RPM is equipped with a computerised temperature and motor control. The control samples are secured on one of the machine support struts, while experimental samples are placed on the inner frame of the clinostat.

#### *Simulated microgravity:*

The RPM is shown in **Figure 2**. One of the first versions was developed by T. Hoson *et al.* [38]. We used a similar system, manufactured by Dutch Space (formerly Fokker Space, Leiden, The Netherlands). The outer frame rotated independently from the inner frame, which caused the samples to move in 3 axis. The rotational movement of both frames was powered by two servomotors. A PC user interface with dedicated software controlled the random movements of the two servomotors with regard to: onset, rate, and duration of rotation. The rotational velocity of both frames was randomised with a maximum of 60°/sec, direction, and interval was set at random. The samples were fixed in the centre of the inner frame; the largest radius was 57.8 mm to the outermost well (residual  $g$  is between  $10^{-3}$  and  $10^{-2}$  g, [34]). The RPM was accommodated in a temperature-controlled incubator set at 37°C [33]. For the experiments the cell layers were washed three times with Phosphate Buffered Saline (PBS) and prepared for further analysis immediately after retrieval from the RPM machine.

#### *Scanning electron microscopy (SEM):*

To assess overall morphology of the fibroblasts, SEM was performed ( $n = 4$ ). Cells were rinsed, fixed for 5 minutes in 2% glutaraldehyde, followed by 5 minutes in 0.1 M sodium-cacodylate buffer (pH 7.4), dehydrated in a graded series of ethanol, and dried in tetramethylsilane to air. Specimens were sputter-coated with gold and examined with a Jeol 6310 SEM (Tokyo, Japan).

#### *Immunofluorescence*

Components of the cytoskeleton were made visible using fluorescent staining techniques. RDF cells, cultured on microgrooved substrata were rinsed in PBS, pH7.2, fixed for 30 minutes in 2% paraformaldehyde, and permeabilised with 1% Triton X100 for 5 min. Filamentous actin was stained with Alexa Fluor 568 phalloidin (Molecular Probes, A-12380, Leiden, The Netherlands) diluted in 1% Bovine Serum Albumin/PBS to block non-specific epitopes. Vinculin was stained with rabbit polyclonal primary antibodies to vinculin (sc-5573, Santa Cruz biotechnology Inc., Santa Cruz, CA, USA), followed by labelling with goat anti-rabbit secondary antibodies IgG with Alexa Fluor 488 (Molecular Probes, A-11034). Finally, the specimens were examined with a Biorad (Hercules, CA, USA) MRC 1024 confocal laser scanning microscope (CLSM) system with a krypton-argon laser at magnification of 40x. The digital immunofluorescence images acquired with the CLSM were loaded into Image J (version 1.5.0, Wayne Rasband, NIH, USA) to create

overlay images. Cytoskeletal components were examined for their overall morphology as well as their orientation with respect to the groove direction.

#### *Image Analysis*

For quantitative image analysis samples were stained with phalloidin-TRITC (Sigma, P-1951, St. Louis, MO, USA), followed by examination with a Leica/Leitz DM RBE Microscope (Wetzlar, Germany) at magnification of 10x. The phalloidin-TRITC fluorescence micrographs were analyzed with Scion Image software (Beta Version 4.0.2, Scion Corp., Frederick, MD, USA). The orientation of fibroblasts was examined and photographed. For each sample six fields of view were selected randomly. The criteria for cell selection were (1) the cell was not in contact with other cells and (2) the cell was not in contact with the image perimeter. The maximum cell diameter was measured as the longest straight line between two edges within the cell borders. The angle between this axis and the grooves (or an arbitrarily selected line for smooth surfaces) was termed the orientation angle. If the average angle was 45 degrees, cells were supposed to have a random orientation. Cell extensions like filopodia, which could confound the alignment measurement, were not included when assessing the cell orientation. Using Clarks criteria [39; 40], cells oriented at 0–10 degrees from the groove direction were regarded to be aligned. The distribution of cytoskeletal patterns with time, gravity force in view of the type of microgrooves and groove direction was described by the percentage of cells in the sample that displayed each pattern. Between 500 and 800 cells were measured per group for both orientation and surface area. Cellular surface area was measured with the aforementioned image analyser software. Applying the same criteria for cell selection; cell areas were determined and displayed as  $\mu\text{m}^2$ . Between 350 - 500 cells were measured per group for both orientation and surface area.

#### *Quantitative-PCR*

Total RNA was isolated from fibroblasts with an RNA isolation and stabilisation kit (QIAGEN, Hilden, Germany) and cDNA was synthesised with reverse transcription in 11  $\mu\text{l}$  aliquots of total RNA with an RT-PCR kit (Invitrogen, Carlsbad, CA, USA).

After RNA isolation and stabilisation and cDNA amplification; 12.5  $\mu\text{l}$  of iQ SYBR Green SuperMix (Bio-Rad, Hercules, CA, USA) was added to each well of an optical 96 wells plate, 1.5  $\mu\text{l}$  of both forward and reverse primer were added, as well as, 4.5  $\mu\text{l}$  DEPC and 5  $\mu\text{l}$  of 10 times diluted cDNA sample. The wells plate was covered and centrifuged shortly to remove air bubbles, following PCR quantification using cycling parameters: 95 °C x3 min; 95 °C x15 seconds → 60 °C x30 seconds followed by 72 °C x30 seconds for 40 cycles. All samples were analysed in triplicate. The comparative Ct-values method was used to calculate the relative quantity of  $\alpha 1$ -,  $\beta 1$ -, and  $\beta 3$ -integrin, and Collagen Type I and GAPDH [41]. Expression of the housekeeping gene glyceraldehyde-3-phosphate dehydrogenase (GAPDH) was used as an internal control to normalise results.

#### *SDS-PAGE and Western Blot analysis*

For preparing total protein extracts; cells were washed 3 times with ice cold PBS. Cells were harvested by scraping followed by disruption with 500  $\mu\text{l}$  ice-cold lysis buffer (50 mM Tris (pH 7.4), 250 mM NaCl, 5 mM EDTA, 50 mM NaF, 1mM  $\text{Na}_3\text{VO}_4$ , 1% Nonidet P40 (BioSource, Camarillo, CA, USA) supplemented with 1 mM Phenylmethanesulfonyl fluoride (PMSF, P7626, Sigma-Aldrich, Steinheim, Germany) and Protease Inhibitor Cocktail (P2714, Sigma-Aldrich). Samples were cleared of cellular debris and concentrated by centrifugation for 65 minutes, 4°C at 12,000 rpm (Amicon Microcon YM-10 centrifugal filter tube, Millipore, Billerica, MA, USA). The protein concentrations in the retentate were determined, and equal amounts of protein were

dissolved in 10µl of 2x reducing sample buffer (4% SDS, 100mM Tris (pH 6.0), 10% β-mercaptoethanol, 20% Glycerol) and heated at 95°C for 5 minutes and electrophoresed on 12.5% SDS-Acrylamide minislab gels and transferred to (polyvinylidene difluoride) PVDF membranes (Immobilon-P, Millipore). After protein transfer, the membranes were blocked in 4% powdered milk in TBST (0.05% Tween 20 in TBS) overnight at room temperature. Immunological blots were then performed at room temperature for 1 hour in 2% skim milk in TBST buffer containing specific primary antibodies (see below).

#### *Antibodies for Western Blot analysis*

Western blots were probed with the following antibodies: Anti-ERK 1/2 (C-16; sc-93), JNK1 (C-17; sc-474), p38 MAPK (C-20; sc-535), αPAK (H-300; sc-11394), RhoA (119; sc-179), Rac1 (T-17; sc-6084), Cdc42 (P1; sc-87). Phosphorylated (i.e. active) proteins were investigated with anti-active p-ERK 1/2 (E-4; sc-7383), p-JNK (G-7; sc-6254), and p-p38 (D-8; sc-7973). All antibodies were obtained from Santa Cruz Biotechnology.

After membranes were washed with TBST, they were incubated with appropriate secondary antibody IgG with alkaline phosphatase conjugate and immunoreactive bands were visualized using Nitroblue Tetrazolium (NBT) and 5-bromo-4-chloro-3-indolyl phosphate (BCIP) chemiluminescence reagents (Bio-Rad Laboratories Hercules, CA, USA).

#### *Statistical analysis:*

Acquired data from the fluorescence micrographs of cell alignment, as well as, QPCR data were analysed using SPSS for Windows (Release 12.0.1, SPSS Inc., Chicago, USA). The effects of and the interaction between both time and/or force and surface were analysed using analysis of variance (ANOVA), including a modified least significant difference (Tukey) multiple range test to detect significant differences between two distinct groups. Probability (p) values of  $\leq 0.05$  were considered significant.

## **RESULTS**

### *Scanning Electron Microscopy*

The microtopography pattern of grooves and ridges was accurately reproduced in the polystyrene substrata. When observing cell morphology, RDFs cultured on smooth substrata showed a cell spreading, which was not only considered random but also displayed the different stages of cell spreading; from round cells with abundance amounts of filopodia to flat stretched out cells with large cell surface areas (**Figure 3A-C**). RDFs seeded onto grooved substrata already showed alignment from an early time point onward although their cell bodies were still rather wide. In later stages the fibroblasts had stretched out into elongated cells with narrow cell width and high alignment (**Figure 3D-F**).

When subjected to simulated microgravity, RDFs cultured on smooth surfaces at first appeared to differ only minimally in cellular behaviour (**Figure 3G**). However, after 120 minutes cells displayed cell membrane ruffles, but retained their spindle shape (**Figure 3H**). After 48 hours fibroblasts appeared as long spindle-shaped cells (**Figure 3I**). RDFs seeded onto grooved surface in the RPM appeared similar in their cell morphology when compared to their 1g counterparts, although cell widths were not as narrow. This became more apparent after 48 hours of culturing under simulated microgravity conditions (**Figure 3J-L**).

### *Fluorescence microscopy (CLSM)*

The cytoskeleton was investigated by staining filamentous actin and vinculin containing anchor points of the cell focal adhesions. **Figure 4A-C** shows 1g smooth substratum samples for 3 time

points; the observed cell shape, spreading, and random orientation were similar to SEM micrographs. Actin filaments (red), were always running in the direction of the long axis of cells. Vinculin staining for focal adhesions resulted in a non-specific staining around the nucleus.

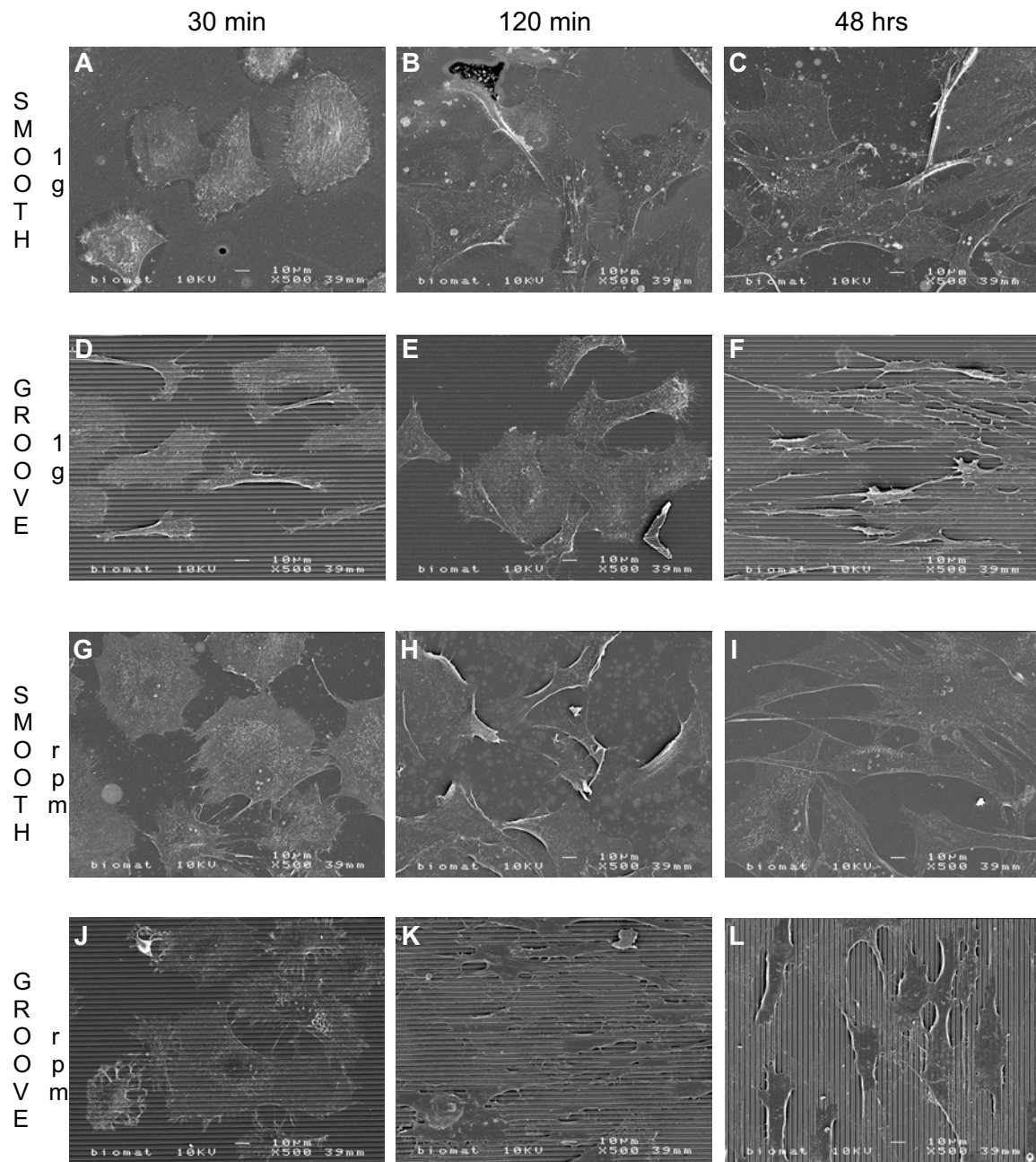


*Figure 3. SEM micrographs of RDFs cultured under various conditions. Normal gravity: (A) Smooth substratum, 30 minutes, (B) Smooth, 120 minutes, (C) Smooth, 48 hours and (D) Grooved surface, 30 minutes, (E) Groove, 120 minutes, (F) Groove, 48 hours. Microgravity: (G) Smooth 30 minutes, (H) Smooth, 120 minutes, (I) Smooth, 48 hours and (J) Groove surface, 30 minutes, (K) Groove, 120 minutes, (L) Groove, 48 hours (magnification x500).*

Vinculin spots (green) were visible in some samples, positioned at the end of actin bundles, and always extended in the direction of the actin bundle. RDFs cultured on grooved surfaces displayed a similar morphology, as found on smooth surfaces; however, there was increased orientation of the cells and their cytoskeleton with time (**Figure 4D-F**).

Cell morphology and cytoskeleton (CSK) distribution of RDFs cultured on smooth substrata in the RPM appeared to remain the same, although after 30 minutes the F-actin bundles seem to be more

pronounced (**Figure 4G**). After 2 hours of RPM, F-actin bundles had become thinner (**Figure 4H**). After 48 hours under simulated weightlessness conditions, RDFs cultured in smooth surfaces appeared in all shapes and sizes, however, elongated cells seemed to be more abundant. Their CSK was clearly defined, and focal adhesion points were lavishly present (**Figure 4I**).

RDFs cultured on grooved substrata in the RPM as shown in **Figure 4J & K** revealed a comparable cellular alignment towards the grooves when compared to the 1g control groups. Fibroblasts cytoskeleton showed round cells with F-actin in the long axis of the cells, and vinculin anchor points at the end of these thick actin bundles. After 48 hours of simulated microgravity cells had recuperated and appeared to be highly aligned, although their cell bodies were wider, as seen in the clearly visible actin filaments and vinculin staining (**Figure 4L**).

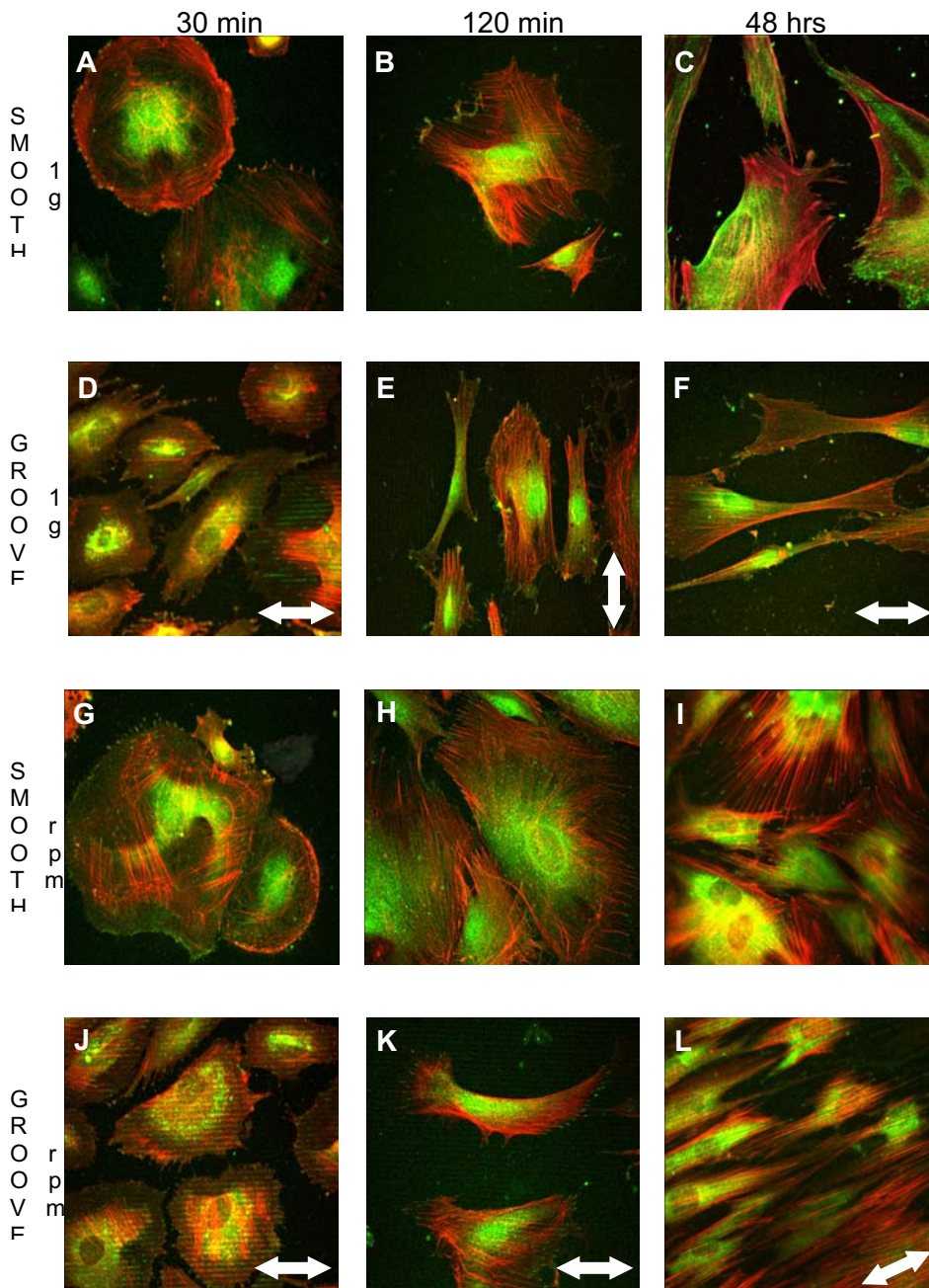


*Figure 4. CLSM micrographs of RDFs cultured under several conditions. Normal gravity: (A) Smooth substratum, 30 minutes, (B) Smooth, 120 minutes, (C) Smooth, 48 hours and (D) Grooved surface, 30 minutes, (E) Groove, 120 minutes, (F) Groove, 48 hours. Simulated microgravity: (G) Smooth 30 minutes, (H) Smooth, 120 minutes, (I) Smooth, 48 hours and (J) Groove surface, 30 minutes, (K) Groove, 120 minutes, (L) Groove, 48 hours. Double ended arrow denotes groove direction. Colour figure on page 166.*

#### *Image Analysis*

Actin filaments were stained with Phalloidin-TRITC and image analysis was conducted, which showed that RDFs orientation was profound on all grooved substrata. RDFs seeded onto smooth

surfaces displayed a random orientation in cell alignment. The quantified results for cellular alignment are presented in **Figure 5**. Within the smooth groups the mean angle remained stable in time and/or gravity, and thus no significant differences were found. There were significant differences between the smooth and grooved groups obviously, but more important were the differences within the grooved groups as was proven by analysis of variance (ANOVA) multiple comparison test. In this analysis the main parameters: topography, gravity, and time proved significant in all but one case.

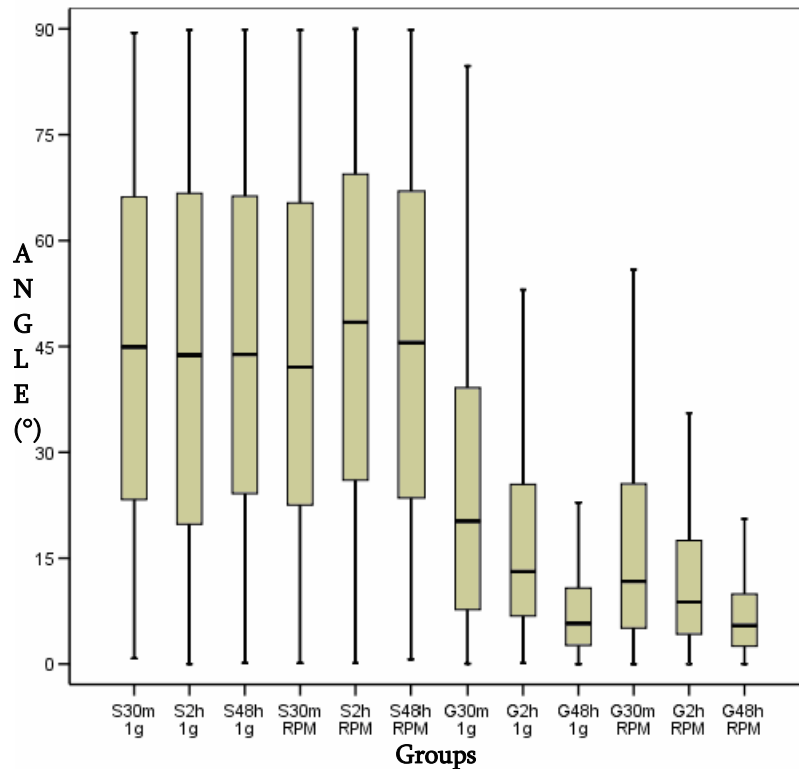


*Figure 5. Box-whisker plot showing the distribution of cellular orientation of fibroblasts under various circumstances of mechanical loading. While the smooth substrata elicit random orientation as seen by the mean angle around 45 degrees, the groove patterns make fibroblast align and with time enhance their orientation towards the grooves as shown by the decreasing mean angle. Within the grooved sample groups all differences in mean angle are significant except those for the 48 hours groups. For each sample at least 500 individual cells were analysed. S = smooth, G = grooved, 30m, 2h, and 48h stands for the experiment time, and 1g and RPM stands for the applied gravitational force.*

Regarding topography, around 80% of the cells cultured on grooved substrata were considered aligned compared to 13% on smooth surfaces.

The effects of gravitational unloading is significant, under simulated microgravity the mean angle of fibroblasts on grooved surfaces decreased compared to 1g control groups, thus the overall alignment increased. Particularly in the earlier time points, cells in the RPM, on average, had a mean angle 6 degrees below that of the 1g control groups, in addition a higher proportion (averaging an additional 20%) of the cells were aligned. After 48 hours there were no significant differences to any further extent between the 1g and RPM grooved groups. The mean angle levelled out to around 8-9 degrees for 80 percent of all fibroblast cells at 48 hours.

Time played an important role in the cellular orientation: 48 hour groups always showed a significantly increased alignment towards the grooves. Up to 80% of cells were aligned after 48 hours compared to 40% and 52% after respectively, 30 and 120 minutes of culturing.

Comparable to the orientation of the RDFs, there was a significant difference in cell area between smooth and grooved substrata, but also among the control and RPM treated groups (**Figure 6**). On grooved surfaces overall cell area was about  $2580 \pm 180 \mu\text{m}^2$  compared to  $3230 \pm 265 \mu\text{m}^2$  overall on smooth surfaces. In the RPM, fibroblasts cultured on smooth surfaces for 30 minutes compared to fibroblasts cultured on grooved surfaces for 30 minutes had a significant difference in cell surface area ( $4267 \pm 530 \mu\text{m}^2$  and  $3345 \pm 242 \mu\text{m}^2$ , respectively). After 48 hours in RPM cell surface area in the grooved groups decreased significantly to  $1798 \pm 175 \mu\text{m}^2$ , while smooth groups settle around  $2968 \pm 295 \mu\text{m}^2$ .

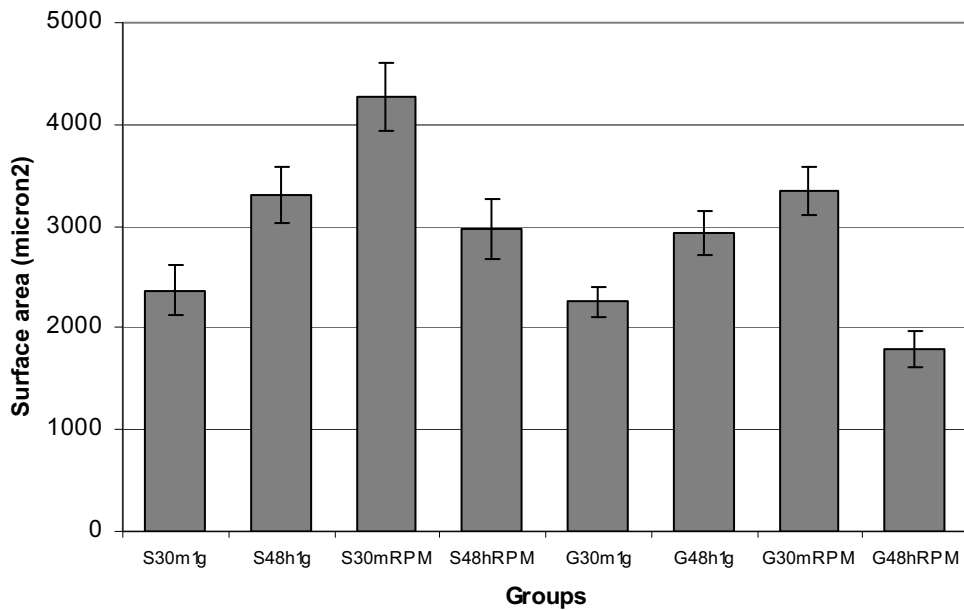


Figure 6. Bar graphs showing the mean and standard error of the for cell surface area of fibroblasts subjected to various parameters. The pattern in both smooth and grooved groups are the same, although the average cell area value for grooved groups is lower. See Figure 5 for explanation of abbreviations.

### Quantitative-PCR

Real-time PCR analysis was performed to quantify the mRNA expression of  $\alpha$ 1-,  $\beta$ 1-, and  $\beta$ 3-integrins, and collagen type I in fibroblasts. **Figure 7** shows the relative changes in gene expression of the various mRNA transcripts. Transcripts were normalised to the internal control gene GAPDH, and were computed relative to the expression in the smooth or the grooved 1g control group.

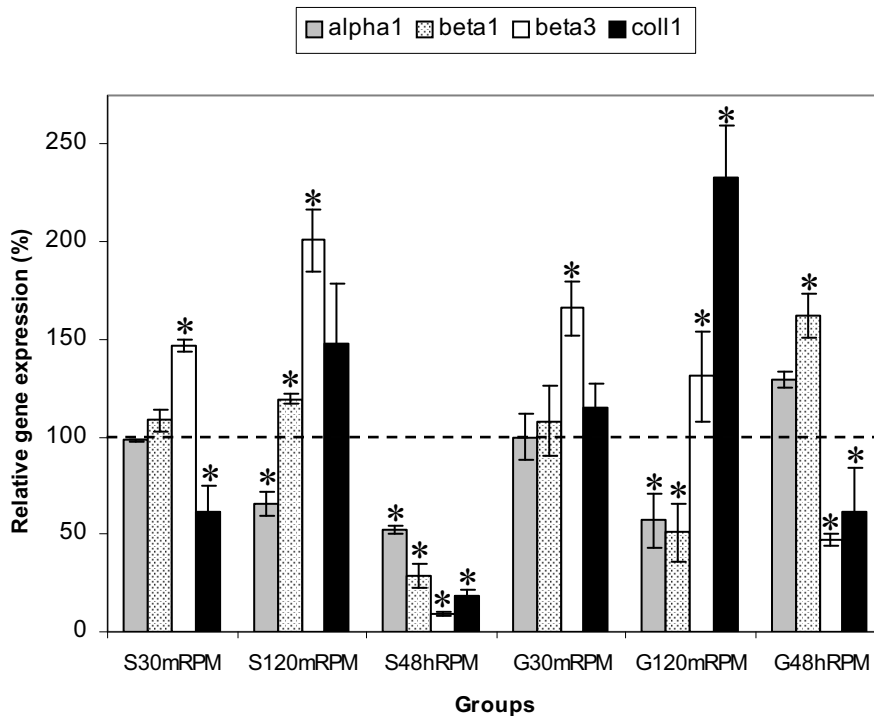


Figure 7. Relative mRNA levels of alpha-1, beta-1, beta-3 integrins, and collagen type I of fibroblast in microgravity setting, cultured for 30 min, 120 min, and 4 hours on either smooth or grooved surfaces. Total RNA was isolated after gravitational loading and Q-PCR performed. For the internal standard the respective 1g smooth or 1g grooved substrate was used. S = Smooth, G = Groove. 30m, 120m, and 48h are the experimental times, and RPM the type of applied gravity. Dashed line represents no difference/control group. Data are expressed as mean  $\pm$  SD, n = 3. \*Significant difference (p < 0.05).

Alpha-1 gene expression in smooth experimental samples was down-regulated from two hours of culturing onward. Beta-1 and beta-3 integrin expression were initially elevated, at 48 hours however, both were significantly decreased. Collagen type I was up-regulated at two hours, after two days gene expression was severely reduced.

Within the grooved groups, alpha-1 integrin expression is down-regulated at first, but is restored after 48 hours. Beta-1 integrin showed a similar pattern. After 2 days of culturing in RPM, beta-1 is significantly up-regulated. Beta-3 integrin expression was initially increased, the last time point showed a significant decrease. Collagen type I gene expression is markedly up-regulated at two hours of experiencing RPM.

#### *SDS-PAGE and Western Blot analysis*

All three major signaling pathways within the Mitogen Activated Protein Kinase (MAPK) pathway were present: ERK-1/2, JNK/SAPK-1/2, and p38 MAPK. Also, their active (phosphorylated) form, could be detected in most groups (**Figure 8 A-C**). ERK-1/2 protein was present in all groups, and particularly in the 1g control groups, active ERK-1/2 protein could be detected in the all groups, although an increase was found after 48 hours in the 1g control group. While p-ERK-1/2 appeared predominantly in the 1g control groups, JNK/SAPK and p38 showed increased presence in both total and active protein in the 0g experiment groups. Especially during the early time points (30 and 120 minutes) larger bands were visible.

Upstream of the ERK pathway, RhoA and ROCK1/2 were detected (**Figure 9A&B**). These proteins, which are important in cell adhesion showed overall an improved presence with an increase in time and a decrease in gravity. Closely linked to RhoA, are Cdc42 and Rac1 fusion protein (**Figure 9 C&D**). These proteins are involved with cell motility and their presence was also increased in time and appeared to be up-regulated under microgravity conditions. PAK protein, a downstream effector of Cdc42 and Rac1, was also present. It appeared more in the grooved substrata groups than smooth, and microgravity resulted in an increase. The detection of PAK was hampered by the fact that the primary antibody not only bound to  $\alpha$ -PAK, but also detected  $\beta$ - and  $\gamma$ -PAK, resulting in a smudged appearance (**Figure 9E**).

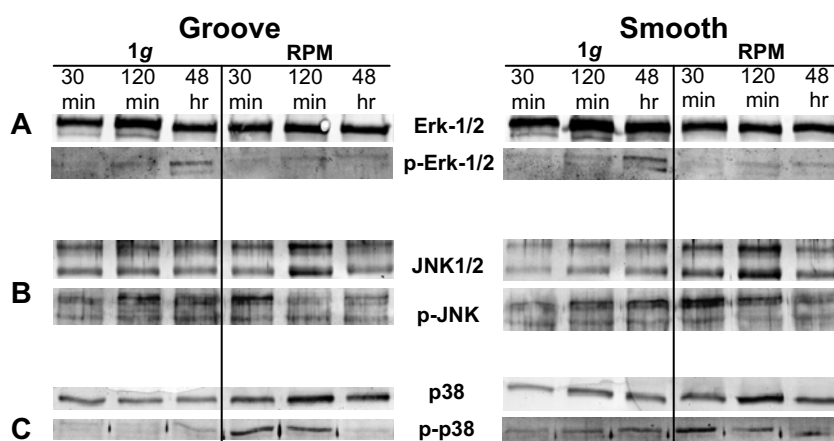


*Figure 8. Western blots analysis of MAPK signalling pathways from whole cell lysates prepared from primary fibroblasts. Equal amount of protein were probed with antibodies specific to total ERK1/2 (A, top row) and phospho-ERK1/2 (A, bottom row) followed by immuno-staining with IgA Alkaline Phosphate conjugate. The whole cell extracts as described in panel A were analyzed by Western blotting. Samples were probed with antibodies specific for total JNK1/2 (B, top row) and phospho-JNK1/2 (B, bottom row), total p38 (C, top row) and phospho-p38 (C, bottom row).*

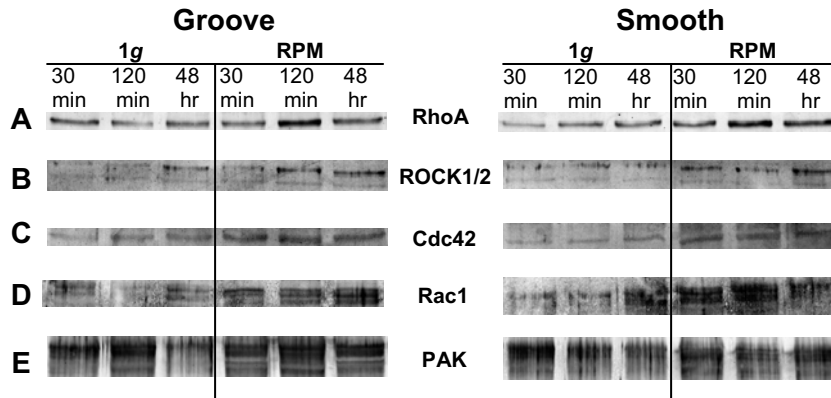


Figure 9. Western blots analysis of small GTPases family members from whole cell extracts prepared from primary fibroblasts. Equal amount of protein were probed with antibodies specific to total RhoA (A), ROCK1/2 (B), Cdc42 (C), Rac1 fusion protein (D), and  $\alpha/\beta/\gamma$ PAK (E) followed by immuno-staining with IgA Alkaline Phosphate conjugate. The whole cell extracts were analyzed by Western blotting.

## DISCUSSION

The aim of this study was to identify what is essential in determining morphological cell response to substrata and simulated microgravity. Fibroblasts were cultured on polystyrene substrata, both smooth and grooved, which were mounted inside the RPM. The mechanotransduction of these forces onto the cells were investigated from several angles: morphological cell responses like shape and orientation, and related to that the cytoskeleton of the cells; as well as the expression of several proteins involved in cell-surface interaction using Q-PCR. Finally, proteins of the MAPK intracellular signalling kinase pathways were visualised. From our data we concluded that RDFs adjust their shape according to micro-topographical features. In addition, microgravity plays a significant role on the cells response to outside environmental factors. Under simulated microgravity in the RPM, cells tend to rely more on the stresses encountered from the remaining environmental parameter, i.e. the substratum. It seems that the grooves enhance the cellular-substratum interface. This is reflected by the presence and/or activation of the several proteins involved in the MAPK pathways which control cell adhesion during exposure to simulated microgravity.

Our random positioning machine model to study microgravity has been reviewed by a number of publications, which have pointed out the usefulness of the RPM as a research tool to simulate space flight conditions in order to elucidate how living systems respond to this impact [10; 34; 42-46]. With a rotation of 60 degrees per second the residual  $g$  is between  $10^{-3}$  and  $10^{-2}$  g. Although an increased distance from the centre of rotation at the same speed will result in increased accelerations at the outer edges of the sample, we made the radial distance from the cell samples to both rotational axis as small as possible and thereby compensating as much as possible for any perception of gravity stimulus. A key principle in RPM use is that by increasing the frequency of rotation the travelling distance gets smaller. By performing this rotation constantly, a circular path is generated and by increasing the rate, cells will rotate around their own axis. This controlled rotation not only applies to the cells but also its surrounding liquid phase. It is argued that the coupling between the cells and the static surrounding liquid is the main reason for this microgravity simulation paradigm [34; 47]. However, a publication by Albrecht-Buehler [48] narrates that a true microgravity characteristic is the absence of buoyancy-driven convective currents. Under weightlessness circumstances, liquid or gaseous regions which have different temperature or composition cannot rely on convective currents to equalise their density and composition. In contrast, they rely on diffusion, which is a very slow process. The rotation of the samples mounted onto the RPM generates internal motion, which increases the mixing of the sample environment comparable to the levels of normal gravity convection. Within the RPM

gravity compensation occurs, which even if completely effective does not remove chronic gravitational stimulation. This stimulation might be perceived by mechanosensors within a cell and could initiate the mechanotransduction process. In attached cells this residual  $g$  may not be regarded as regular gravity applied to the cells. It is in fact an inertial shear force and directed perpendicular as compared to gravity generated by Earth. Cells undergoing RPM might display a small, perhaps significant, displacement of their total mass or intracellular structures [34].

True zero  $g$ , that is not to experience any gravitational pull, can only be achieved if an object would be infinitely far from any gravitating body (gravity may be a weak force; however, it has a long reach). All other conditions of weightlessness result from a net sum of all present forces equalling zero, not from an absence of gravity. This is impossible to achieve; we can only effectively isolate an experiment from the attraction of gravity while remaining in our solar system. Since attraction decreases non-linearly with increasing distance from the source, even a spacecraft in Low Earth Orbit experiences approximately 90% of the gravitational acceleration that exists at the surface of the Earth. From an analytical point of view regarding the RPM, it is necessary to identify all relevant gravity dependent variables in the system in order to resolve the extent to which the altered inertial environment created via rotation mimics the specific underlying cause-and-effect interactions that occur in a weightlessness environment [47]. However, from a researcher's perspective it might be better if efforts are spent in optimizing the system in order to attain a better end product. In our study all samples received identical treatment before the start of the experiment and were randomised for RPM or control. Also, to prevent shear stress caused by air bubbles within the contained surroundings of the cell culture which can be disastrous for cell viability [49-51], we used silicone closing caps which attached snug on each well/insert combination. This resulted in the absence of air bubbles before and after rotation. Nevertheless, essential results obtained with the RPM as a simulated microgravity model would ideally have to be confirmed via space experiments.

Combined with previous work [52], several interesting observations concerning cellular alignment on microgrooved topography can be made: within the first 4 hours after cell adhesion, fibroblast orientation rapidly increases. Cells demonstrate a mean angle as low 5 degrees. Fibroblasts in a simulated microgravity environment perform better than those cultured under normal gravity values. On average, cells in the RPM have mean angles around 14°; 6 degrees lower than the 1g control groups. Nevertheless, from 24 hours onward no difference can be distinguished between both 1g and RPM groups. Mean angles of fibroblasts after 48 hours of culturing on microgrooved surfaces, slightly increases before levelling off to 8 degrees.

QPCR data on proteins which are involved in cellular adhesion revealed an interesting development: collagen type I, an ECM component as deposited by the cells in order to adhere to their environment, was greatly reduced in samples run experiencing simulated microgravity conditions, as opposed to control (1g) samples. This seems to contradict Seitzer *et al.* [53], who reported an increase in collagen synthesis by fibroblasts cultured on thermanox coverslips under real microgravity conditions. However, they also showed that after 20 hours of culturing this increase was reduced to 10% compared to control samples. In previous research we have shown that prolonged culturing will counteract such up-regulations [52], which corroborates with Saito *et al.* [16] who also observed an decrease of collagen synthesis (both mRNA and protein) by osteoblast-like cells after 72 hours of simulated microgravity.

The up-regulation of beta-3 integrin of fibroblasts which underwent simulated microgravity during the early stages underscores that this subunit is an important functional receptor for ECM components (e.g., collagen). Combined with alpha-1 subunits, this beta-3 integrin mediates cell spreading on fibrillar type I collagen [54]. Recent studies [55; 56] observed that talin, an intracellular protein involved in focal adhesion anchorage, which binds to the beta-3 integrin

cytoplasmic tails is directly responsible for “inside-out” activation of beta-3. Quiescence of stable adhered cells might result in a slow recycling of integrins and explain that after 48 hours the beta-3 expression plummets in favour of beta-1 integrin, which throughout the different groups remained by and large unchanged or slightly elevated. The notable exception in beta-3 integrin gene expression occurs in cells cultured for 48 hours under RPM conditions, there beta-3 are severely down-regulated. This performance of beta-1, and alpha-1, corresponds with previous work [52; 57] and denotes the importance of these subunits in long-term interaction between a cell and its environment.

Elevated phosphorylation levels of JNK/SAPK and p38 indicate that these two major pathways, which are commonly activated by stressful conditions, were also activated by microgravity. As mentioned below, upstream  $\alpha/\beta/\gamma$ PAK which activates JNK is also increased under RPM conditions. Upstream to PAK, the small GTPases Rac, Cdc42 also expresses increased activation after microgravity exposure.

Total ERK1/2 did not change for cells cultured on groove patterns under simulated microgravity. Although it could be argued that a small reduction exists for total ERK1/2 on the smooth substrate, it is clear that phosphorylated-ERK1/2 is obviously reduced in both the planar and the topographic surfaces. Meyers *et al.* [57] also reported ERK reduction in osteoblast cells; there the discontinued activation of ERK1/2 affected the Runx2 activation, an essential transcription factor for osteoblastic differentiation. Active-ERK1/2 in fibroblast cells is required for growth-factor-induced cell motility responses. A reduction might suggest that cells hunker down and stop moving altogether. This leads to increased surface area on these substrates, which increases the probability of fibroblasts forming stable attachments. This increase in adhesion results in more intracellular signaling cascades, which is reflected by an increase in activity of the members of the Rho GTPases family during exposure to simulated microgravity. This increase is present throughout, and demonstrates the interactions which exist at this intracellular level. It also reveals that fibroblasts are actively engaged with their environment. The morphological appearance of fibroblasts in the RPM underscores this observation: cells are outstretched, and display a proper cytoskeleton, however an increase in vinculin anchor points around the nucleus is also visible and fibroblast cell shape under zero g is markedly different compared to their 1g control counterparts.

## CONCLUSIONS

There are suggestions that mechanical and physical forces may be sensed at the outset as local deformations or stimulation of the cell surface and those mechano-sensitive systems might promote changes in cell-signalling pathways, which are transformed subsequently into molecular responses. Another point of view is that the triggering element results from the intracellular polarised displacement of their total mass or intracellular structures/components. Notwithstanding the nature of the sensors, the “impact” of weightlessness is probably related narrowly to the functional state of cell membranes and contractible elements of the cytoskeleton. The involvement of these cell components may be crucial in the processes of reception and realisation of gravitational stimuli, as demonstrated by the clear alterations in the molecular organization of membranes and cytoskeleton under altered gravity conditions on a variety of cells.

Our results are consistent with the aforementioned observation that utilisation of microgravity to primary fibroblast cells encourages them to change their morphological appearance, and their expression of cell-substratum proteins through the MAPK intracellular signalling pathways. Our hypothesis is partially true: cells do orientate along the grooves, however simulated microgravity enhances fibroblast orientation on grooved substrates.

## REFERENCES

1. Walboomers, X. F., Croes, H. J., Ginsel, L. A., and Jansen, J. A. Growth behavior of fibroblasts on microgrooved polystyrene. *Biomaterials* 1998, 1861-1868, 1998.
2. den Braber, E. T., de Ruijter, J. E., Smits, H. T., Ginsel, L. A., von Recum, A. F., and Jansen, J. A. Quantitative analysis of cell proliferation and orientation on substrata with uniform parallel surface micro-grooves. *Biomaterials* 1996, 1093-9, 1996.
3. Clark, P., Connolly, P., Curtis, A. S., Dow, J. A., and Wilkinson, C. D. Cell guidance by ultrafine topography in vitro. *J Cell Sci* 1991, 73-7, 1991.
4. Ingber, D. E. Tensegrity I. Cell structure and hierarchical systems biology. *J Cell Sci* 2003, 1157-73, 2003.
5. Ingber, D. E. Integrins, tensegrity, and mechanotransduction. *Gravit Space Biol Bull* 1997, 49-55, 1997.
6. Curtis, A. and Wilkinson, C. New depths in cell behaviour: reactions of cells to nanotopography. *Biochem Soc Symp* 1999, 15-26, 1999.
7. Brunette, D. M. and Chehroudi, B. The effects of the surface topography of micromachined titanium substrata on cell behavior in vitro and in vivo. *J Biomech Eng* 1999, 49-57, 1999.
8. Oakley, C., Jaeger, N. A., and Brunette, D. M. Sensitivity of fibroblasts and their cytoskeletons to substratum topographies: topographic guidance and topographic compensation by micromachined grooves of different dimensions. *Exp Cell Res* 1997, 413-24, 1997.
9. Chou, L., Firth, J. D., Uitto, V. J., and Brunette, D. M. Substratum surface topography alters cell shape and regulates fibronectin mRNA level, mRNA stability, secretion and assembly in human fibroblasts. *J Cell Sci* 1995, 1563-73, 1995.
10. Uva, B. M., Masini, M. A., Sturla, M., Prato, P., Passalacqua, M., Giuliani, M., Tagliaferro, G., and Strollo, F. Clinorotation-induced weightlessness influences the cytoskeleton of glial cells in culture. *Brain Res* 2002, 132-9, 2002 .
11. Schwarzenberg, M., Pippia, P., Meloni, M. A., Cossu, G., Cogoli-Greuter, M., and Cogoli, A. Signal transduction in T lymphocytes--a comparison of the data from space, the free fall machine and the random positioning machine. *Adv Space Res* 1999, 793-800, 1999.
12. Cogoli, A. and Cogoli-Greuter, M. Activation and proliferation of lymphocytes and other mammalian cells in microgravity. *Adv Space Biol Med* 1997, 33-79, 1997.
13. Rijken, P. J., Boonstra, J., Verkleij, A. J., and de Laat, S. W. Effects of gravity on the cellular response to epidermal growth factor. *Adv Space Biol Med* 1994, 159-88, 1994.
14. Schatten, H., Lewis, M. L., and Chakrabarti, A. Spaceflight and clinorotation cause cytoskeleton and mitochondria changes and increases in apoptosis in cultured cells. *Acta Astronaut* 2001, 399-418, 2001.
15. Grigoryan, E. N., Anton, H. J., and Mitashov, V. I. Microgravity effects on neural retina regeneration in the newt. *Adv Space Res* 1998, 293-301, 1998.
16. Saito, M., Soshi, S., and Fujii, K. Effect of hyper- and microgravity on collagen post-translational controls of MC3T3-E1 osteoblasts. *J Bone Miner Res* 2003, 1695-1705, 2003.
17. Arase, Y., Nomura, J., Sugaya, S., Sugita, K., Kita, K., and Suzuki, N. Effects of 3-D clino-rotation on gene expression in human fibroblast cells. *Cell Biol Int* 2002, 225-33, 2002.
18. Boonstra, J. Growth factor-induced signal transduction in adherent mammalian cells is sensitive to gravity. *FASEB J* 1999, S35-42, 1999.

19. Wang, J. H., Yang, G., Li, Z., and Shen, W. Fibroblasts responses to cyclic mechanical stretching depend on cell orientation to the stretching direction. *J Biomech* 2003, 573-6, 2003.
20. Sciola, L., Cogoli-Greuter, M., Cogoli, A., Spano, A., and Pippia, P. Influence of microgravity on mitogen binding and cytoskeleton in Jurkat cells. *Adv Space Res* 1999, 801-5, 1999.
21. Loesberg, W. A., Walboomers, X. F., van Loon, J. J., and Jansen, J. A. The effect of combined cyclic mechanical stretching and microgrooved surface topography on the behavior of fibroblasts. *J Biomed Mater Res A* 2005, 723-732, 2005.
22. Searby, N. D., Steele, C. R., and Globus, R. K. Influence of increased mechanical loading by hypergravity on the microtubule cytoskeleton and prostaglandin E2 release in primary osteoblasts. *Am J Physiol Cell Physiol* 2005, C148-158, 2005.
23. Aplin, A. E. and Juliano, R. L. Integrin and cytoskeletal regulation of growth factor signaling to the MAP kinase pathway. *J Cell Sci* 1999, 695-706, 1999.
24. Yuge, L., Hide, I., Kumagai, T., Kumei, Y., Takeda, S., Kanno, M., Sugiyama, M., and Kataoka, K. Cell differentiation and p38(MAPK) cascade are inhibited in human osteoblasts cultured in a three-dimensional clinostat. *In Vitro Cell Dev Biol Anim* 2003, 89-97, 2003.
25. Nebreda, A. R. and Porras, A. p38 MAP kinases: beyond the stress response. *Trends Biochem Sci* 2000, 257-260, 2000.
26. Porras, A., Zuluaga, S., Black, E., Valladares, A., Alvarez, A. M., Ambrosino, C., Benito, M., and Nebreda, A. R. P38 alpha mitogen-activated protein kinase sensitizes cells to apoptosis induced by different stimuli. *Mol Biol Cell* 2004, 922-933, 2004.
27. Tang, Y., Yu, J., and Field, J. Signals from the Ras, Rac, and Rho GTPases converge on the Pak protein kinase in Rat-1 fibroblasts. *Mol Cell Biol* 1999, 1881-1891, 1999.
28. He, H., Pannequin, J., Tantiogco, J. P., Shulkes, A., and Baldwin, G. S. Glycine-extended gastrin stimulates cell proliferation and migration through a Rho- and ROCK-dependent pathway, not a Rac/Cdc42-dependent pathway. *Am J Physiol Gastrointest Liver Physiol* 2005, G478-488, 2005.
29. Lim, L., Manser, E., Leung, T., and Hall, C. Regulation of phosphorylation pathways by p21 GTPases. The p21 Ras-related Rho subfamily and its role in phosphorylation signalling pathways. *Eur J Biochem* 1996, 171-185, 1996.
30. Manser, E. Small GTPases take the stage. *Dev Cell* 2002, 323-328, 2002.
31. Mesland, D. A. Mechanisms of gravity effects on cells: are there gravity-sensitive windows? *Adv Space Biol Med* 1992, 211-28, 1992.
32. Hoson, T., Kamisaka, S., Buchen, B., Sievers, A., Yamashita, M., and Masuda, Y. Possible use of a 3-D clinostat to analyze plant growth processes under microgravity conditions. *Adv Space Res* 1996, 47-53, 1996.
33. Mesland, D. A. Novel ground-based facilities for research in the effects of weight. *ESA Microgravity News* 1996, 5-10, 1996.
34. van Loon, J. J. W. A. Some history and use of the random positioning machine, RPM, in gravity relayed research. *Advances in Space Research* 2007, 2007.
35. Chesmel, K. D. and Black, J. Cellular responses to chemical and morphologic aspects of biomaterial surfaces. I. A novel in vitro model system. *J Biomed Mater Res* 1995, 1089-1099, 1995.
36. Freshney, R. I. Culture of animal cells: a multimedia guide. 99. Chichester, John Wiley & Sons Ltd.

37. Walboomers, X. F., Ginsel, L. A., and Jansen, J. A. Early spreading events of fibroblasts on microgrooved substrates. *J Biomed Mater Res* 2000, 529-534, 2000.
38. Hoson, T., Kamisaka, S., Masuda, Y., and Sievers, A. Changes in plant growth processes under microgravity conditions simulated by a three-dimensional clinostat. *Botanical Mag* 1992, 53-70, 1992.
39. Clark, P., Connolly, P., Curtis, A. S., Dow, J. A., and Wilkinson, C. D. Topographical control of cell behaviour: II. Multiple grooved substrata. *Development* 1990, 635-644, 1990.
40. Clark, P., Connolly, P., Curtis, A. S., Dow, J. A., and Wilkinson, C. D. Topographical control of cell behaviour. I. Simple step cues. *Development* 1987, 439-448, 1987.
41. Livak, K. J. and Schmittgen, T. D. Analysis of relative gene expression data using real-time quantitative PCR and the 2<sup>(-Delta Delta C(T))</sup> Method. *Methods* 2001, 402-8, 2001.
42. Cogoli, M. The fast rotating clinostat: a history of its use in gravitational biology and a comparison of ground-based and flight experiment results. *ASGSB Bull* 1992, 59-67, 1992.
43. Villa, A., Versari, S., Maier, J. A. M., and Bradamante, S. Cell behaviour in simulated microgravity: a comparison of results obtained with RWV and RPM. *Grav Space Biol* 2005, 89-90, 2005.
44. Kraft, T. F., van Loon, J. J., and Kiss, J. Z. Plastid position in Arabidopsis columella cells is similar in microgravity and on a random-positioning machine. *Planta* 2000, 415-22, 2000.
45. Vassy, J., Portet, S., Beil, M., Millot, G., Fauvel-Lafeve, F., Karniguian, A., Gasset, G., Irinopoulou, T., Calvo, F., Rigaut, J. P., and Schoevaert, D. The effect of weightlessness on cytoskeleton architecture and proliferation of human breast cancer cell line MCF-7. *FASEB J* 2001, 1104-6, 2001.
46. Hughes-Fulford, M. Signal transduction and mechanical stress. *Sci STKE* 2004, RE12, 2004.
47. Klaus, D. M. Clinostats and bioreactors. *Gravit Space Biol Bull* 2001, 55-64, 2001.
48. Albrecht-Buehler, G. The simulation of microgravity conditions on the ground. *ASGSB Bull* 1992, 3-10, 1992.
49. Hammond, T. G. and Hammond, J. M. Optimized suspension culture: the rotating-wall vessel. *Am J Physiol Renal Physiol* 2001, F12-25, 2001.
50. Cherry, R. S. and Hulle, C. T. Cell death in the thin films of bursting bubbles. *Biotechnol Prog* 1992, 11-8, 1992.
51. Kleis, S. J., Schreck, S., and Nerem, R. M. A viscous pump bioreactor. *Biotech Bioeng* 1990, 771-777, 1990.
52. Loesberg, W. A., Walboomers, X. F., Bronkhorst, E. M., van Loon, J. J., and Jansen, J. A. The effect of combined simulated microgravity and microgrooved surface topography on fibroblasts. *Cell Motil Cytoskeleton* 2007, 174-185, 2007.
53. Seitzer, U., Bodo, M., Muller, P. K., Acil, Y., and Batge, B. Microgravity and hypergravity effects on collagen biosynthesis of human dermal fibroblasts. *Cell Tissue Res* 1995, 513-7, 1995.
54. Jokinen, J., Dadu, E., Nykvist, P., Kapyla, J., White, D. J., Ivaska, J., Vehvilainen, P., Reunanen, H., Larjava, H., Hakkinen, L., and Heino, J. Integrin-mediated cell adhesion to type I collagen fibrils. *J Biol Chem* 2004, 31956-63, 2004.
55. Nayal, A., Webb, D. J., and Horwitz, A. F. Talin: an emerging focal point of adhesion dynamics. *Curr Opin Cell Biol* 2004, 94-8, 2004.
56. Zou, Z., Chen, H., Schmaier, A. A., Hynes, R. O., and Kahn, M. L. Structure-function analysis reveals discrete beta3 integrin inside-out and outside-in signaling pathways in platelets. *Blood* 2007, 3284-3290, 2007.

57. Meyers, V. E., Zayzafoon, M., Gonda, S. R., Gathings, W. E., and McDonald, J. M. Modeled microgravity disrupts collagen I/integrin signaling during osteoblastic differentiation of human mesenchymal stem cells. *J Cell Biochem* 2004, 697-707, 2004.